Nutrient enrichment, habitat variability and trophic transfer efficiency in simple models of pelagic ecosystems

W. M. Kemp*, M. T. Brooks, R. R. Hood

University of Maryland, Center for Environmental Science, Horn Point Laboratory, PO Box 775, Cambridge, Maryland 21613, USA

ABSTRACT: We developed 4 simple numerical models of plankton dynamics to explore how nutrient enrichment and habitat variability might influence the efficiency by which phytoplankton (P) production is transferred to growth of zooplankton (Z) consumers in coastal ecosystems. The 4 models range in complexity from 2 (P and Z) to 5 state variables (including detritus, nutrients, and 2 algal size-groups). The models employ generic equation formulations, which are generally well supported by empirical studies and are widely used in coastal ecosystem modeling. Simulation experiments revealed that trophic transfer efficiency (TTE = zooplankton growth per unit phytoplankton production) tends to be enhanced with increased variability of resources, particularly at low nutrient levels. Numerical and analytical studies also showed that, regardless of resource variability, these model formulations produce a trend of initial enhancement of trophic efficiency with increasing nutrient levels, followed by a marked reduction in efficiency beginning at moderately eutrophic conditions. This precipitous drop in trophic efficiency is attributable to a saturation of the ability of zooplankton to utilize the increased primary production associated with nutrient enrichment. Under these conditions, an increasing fraction of the primary production is shunted to microbial food chains and associated respiratory losses. The steepness of this reduction in trophic efficiency with nutrient enrichment is related to the strength of predation (or disease) control at upper trophic levels. Model formulations simulating more intense top-down control (i.e. increasing mortality rates with increasing Z abundance) resulted in sharper declines in TTE with increasing nutrients. We speculate that these model results may help to explain how observed reductions in relative fish yield (per unit primary production) in many shallow nutrient-enriched estuaries and lakes are related to interacting effects of cultural eutrophication and intense fisheries exploitation. Furthermore, we surmise that these relationships are robust characteristics of most existing aquatic ecosystem models.

KEY WORDS: Trophic efficiency · Eutrophication · Simulation models · Pelagic ecosystems · Top-down control

INTRODUCTION

A question of long-standing concern in ecology is the amount of fish harvest that can be derived from primary production in aquatic systems (e.g. Oglesby 1977, Nixon 1988). To address this question it is essential to quantify 2 key characteristics of an ecosystem's food web: (1) the efficiency of transfer between each trophic level, and (2) the average number of trophic transfers between primary producers and the fish of interest (e.g. Ryther 1969). The ratio of fish production to primary production, which is constrained by both these mechanisms, is a measure of the ecosystem's trophic transfer efficiency (TTE). These simple relationships have formed the basis for several estimates of potential regional and global fish production in the sea (e.g. Ryther 1969) and for resulting concerns about the

*E-mail: kemp@hpl.umces.edu

sustainability of current harvests (e.g. Pauly & Christensen 1995). Such estimates are, however, critically dependent upon assumptions about TTE between steps in the food chain and how this efficiency changes as a function of nutrient inputs and environmental conditions.

Recent studies have suggested that the ratio of marine fisheries harvest to primary production tends to increase directly with increasing primary production under nutrient-poor conditions but saturates with increased nutrient levels and associated productivity (Iverson 1990). Analyses of global fisheries data, however, indicate that increased fish yield in highly productive ecosystems may, in fact, derive from harvesting organisms at lower trophic levels rather than simply from higher rates of primary production transferred to upper trophic levels with invariant efficiencies (Pauly et al. 1998). Thus, it remains unclear how trophic efficiency supporting fish production actually varies with changes in primary production and nutrient availability. Explanation for such relationships is further complicated by the fact that fish harvesting itself can alter food-web structure through trophic cascades (e.g. Carpenter et al. 1985), thereby potentially modifying overall trophic efficiency.

There is growing evidence from studies of lakes and estuaries that, in some instances, sustainable harvests of fish populations at upper trophic levels may remain constant or even decline as these aquatic ecosystems become highly eutrophic (e.g. Beeton 1969, Caddy 1993). Although it has been suggested that environmentally controlled changes in plankton community structure may alter trophic efficiencies (e.g. Landry 1977, Edmondson 1991), broad quantitative explanations for these postulated relationships between TTE and nutrient enrichment are generally lacking. This uncertainty is disturbing in the light of 2 parallel worldwide trends of increases in both exploitation rates of fish populations (Pauly et al. 1998) and nutrient enrichment in marine and freshwater ecosystems (e.g. Nixon 1995).

In addition to any relationships between trophic efficiency and mean nutrient conditions, recent experiments have indicated that trophic efficiencies of planktonic herbivores may be enhanced by small-scale patchiness of phytoplankton distributions in aquatic ecosystems (e.g. Dagg 1977, Saiz et al. 1993). Thus, zooplankton feeding efficiency might be largely controlled by the spatial-temporal variabilities of nutrients and algae that characterize most lacustrine, estuarine and marine environments (e.g. Mackas et al. 1985). Numerical and analytical computations have been used to illustrate how specific relationships between zooplankton growth efficiency and prey variability depend on physiological, behavioral and physical parameters (e.g. Davis et al. 1991, Tiselius et al. 1993). Other models

have addressed questions of how nutrient variability influences patterns of resource utilization in plankton communities (e.g. Powell & Richerson 1985).

Numerical simulation models have, in fact, been widely used to explore many aspects of trophic dynamics and nutrient cycling in pelagic ecosystems (e.g. Pace et al. 1984, Scavia et al. 1988). Such modeling studies have explored interactions between nutrient availability (bottom-up) and predation rates (top-down) as controls on plankton community structure and production (e.g. Carpenter & Kitchell 1984, Ross et al. 1993a,b). In general, the structure of these models tends to converge on a few common formulations derived from empirical studies (e.g. Scavia 1979, Totterdell 1993). In some cases, however, relatively minor changes in equation form can lead to markedly different simulation behaviors (e.g. Steele & Henderson 1992, Edwards & Brindley 1999). In many cases, highly simplified analytical and numerical models have also proven useful for understanding complex dynamics observed in natural pelagic ecosystems (e.g. Scheffer 1991). Surprisingly little attention has been paid in such pelagic modeling studies, however, to how trophic efficiencies respond to environmental changes. Thus, the purpose of the present paper is to use simulation models for investigating how TTE is altered through changes in inputs and variability of nutrients in pelagic habitats.

METHODS

Model structure and simulations. For this analysis, we developed a family of 4 simple models of pelagic ecosystem dynamics ranging in complexity from 2 to 5 state variables (Fig. 1). Here we describe the structure of the most complex version, which contains 5 compartments (Fig. 1d): dissolved inorganic nitrogen ($N = NH_4^+ + NO_3^- + NO_2^-$); herbivorous zooplankton (Z); large phytoplankton such as diatoms (P_l); small phytoplankton (P_s), and detritus (D). The other 3 models were derived by simplifying and aggregating this 5-compartment model (N-P_l-P_s-Z-D) into models containing 4 (N-P-Z-D), 3 (N-P-Z) and 2 (P-Z) state variables (Fig. 1a–c). The equation terms describing interactions in all 4 plankton models are identical (Table 1), with only minor coefficient adjustments made to account for addition or deletion of pathways (Table 2). The description that follows relates specifically to the 5-compartment model (Fig. 1d). The source code for these models is available upon request from the authors.

We structured this model with a system of 5 finite-difference equations (Table 1), which were calibrated in nitrogen units (μM). We employed conventional equation formulations, the basis for which are described

a) P-Z Model

b) N-P-Z Model
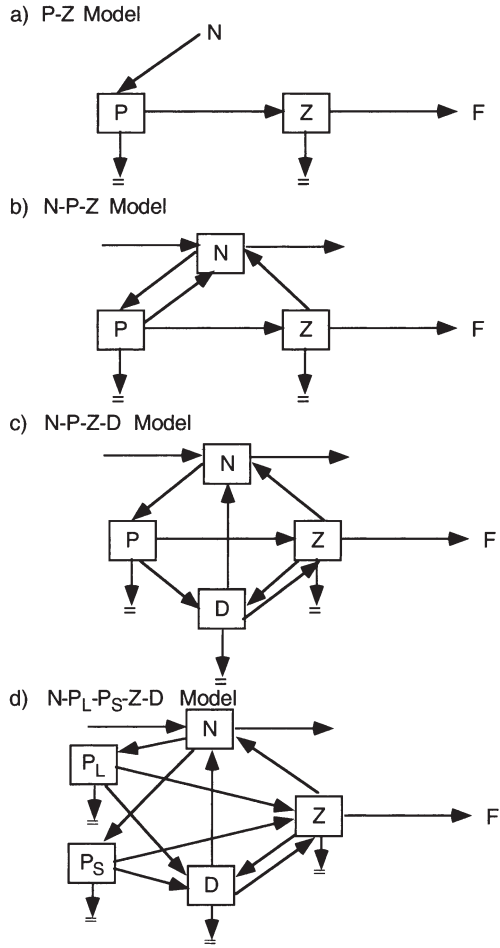
c) N-P-Z-D Model

d) N-P_L-P_S-Z-D Model

Fig. 1. Schematic for 4 versions of a pelagic ecosystem model, with state variables indicated by boxes and trophic pathways and nutrient fluxes by arrows. State variables = P: phytoplankton (subscripts indicate mean cell size, where L = large and S = small); Z: herbivorous zooplankton; N: dissolved inorganic nitrogen; D: detrital organic nitrogen (dissolved and particulate); F: zooplanktivorous fishes. Arrows with double underlining indicate respiration and imply N recycling

Table 1. Differential equations for 5-compartment model of plankton trophic dynamics (N: dissolved inorganic nitrogen; D: detritus; P_l: large phytoplankton; P_s: small phytoplankton; Z: herbivorous zooplankton). All state variables are computed in units of µmol N l^{-1}, and rates are in µmol N l^{-1} d^{-1}. Abbreviations for rates and coefficients are defined in Table 2. Terms are presented in Eqs (1) to (8) and are explained in text

Finite difference equations

$dN/dt = R_Z + R_s + R_l + R_D + Q_I - U_l - U_s - Q_O$

$dD/dt = M_l + M_s + M_Z + Q_I + D_Z - G_D - R_D - Q_O - S_D$

$dP_l/dt = U_l + Q_I - M_l - G_l - R_l - Q_O - S_l$

$dP_s/dt = U_s + Q_I - M_s - G_s - R_s - Q_O$

$dZ/dt = G_l + G_s + G_D + Q_I - M_Z - R_Z - Q_O - D_Z$

Respiration and excretion (R) rates

$R_z = [(\xi_{a_l} - \xi_{g_l}) \cdot G_l] + [(\xi_{a_D} - \xi_{g_D}) \cdot G_D] + [(\xi_{a_s} - \xi_{g_s}) \cdot G_s]$

$R_l = (1 - b) \cdot (l_l \cdot P_l^2)$

$R_s = (1 - b) \cdot (l_s \cdot P_s^2)$

$R_d = r \cdot D$

Mortality (M) and defecation (d) rates

$M_l = b \cdot l_l \cdot (P_l)^2$

$M_s = b \cdot l_s \cdot (P_s)^2$

$M_Z = p_z \cdot (Z)^2$

$d_Z = [(1 - \xi_{a_l}) \cdot G_l] + [(1 - \xi_{a_s}) \cdot G_s] + [(1 - \xi_{a_D}) \cdot G_D]$

Zooplankton grazing (G) rates

$G_l = [G_{max} \cdot Z \cdot \beta_1 \cdot (P_1 - \alpha)]/[(\beta_1 \cdot P_1) + (\beta_s \cdot P_s) + (\beta_D \cdot D) + K_Z]$

$G_s = (G_{max} \cdot Z \cdot \beta_s \cdot P_s)/[(\beta_1 \cdot P_1) + (\beta_s \cdot P_s) + (\beta_D \cdot D) + K_Z]$

$G_D = (G_{max} \cdot Z \cdot \beta_D \cdot D)/[(\beta_1 \cdot P_1) + (\beta_s \cdot P_s) + (\beta_D \cdot D) + K_Z]$

Phytoplankton uptake (U) rates

$U_l = \mu_{max} \cdot [1 - \exp(-I/I_k)] \cdot [N/(N + K_{N_l})] \cdot P_l$

$U_s = \mu_{max} \cdot [1 - \exp(-I/I_k)] \cdot [N/(N + K_{N_s})] \cdot P_s$

Sinking (S) rates

$S_l = v_l \cdot P_l$

$S_s = v_s \cdot P_s$

$S_D = v_D \cdot D$

below, with other details provided elsewhere (Stickney et al. 2000). External forcing functions driving the model included insolation, water-exchange rates and external concentrations of N. The water-exchange rates allowed a constant flow of new nutrients into the system while removing a constant proportion of each state variable per unit time. In the 3- to 5-compartment models, we used external inputs of N to drive the model, while the 2-compartment version had no N state variable, so that phytoplankton assimilated nutrients directly from an external pool.

We developed these models and conducted numerical simulation experiments using Stella II computer software (High Performance Systems Inc., Version 4.0). For all simulations, here, we used a time-step of 0.1 d

and a fourth-order Runga-Kutta numerical integration scheme. Model simulations were conducted under a range of nutrient input conditions and run until steady-state levels were achieved, at which point values for state variables and flows were recorded. In some numerical experiments, nutrient resource patchiness and pulsing were simulated using the Stella built-in function NORMAL, which produces a set of normally distributed random numbers with a given mean and standard deviation. The computed steady-state values of the state variables (with constant nutrient input) were used as initial conditions for simulations with variable nutrient inputs, for comparison purposes. Model behavior was measured primarily in terms of the TTE, which is defined here as the ratio of zooplankton grazing to phytoplankton productivity for full model simulations:

$$\text{TTE} = (\Sigma G_i)/(\Sigma U_j) \qquad (1)$$

where G and U are defined in Table 1, and i and j represent counting variables for food items in Z diet and P groups, respectively.

Phytoplankton. We purposely structured the 5-compartment model so that nutrient levels might alter TTE by modifying mean food-chain length. We did this by setting coefficients for nutrient kinetics so that small algae (P_s) would dominate phytoplankton biomass at low N concentrations and large cells (P_l) would tend to be dominant at high N. This is a realistic representation of the switch that commonly occurs from small to large phytoplankton dominance with increasing nutrient levels (e.g. Scavia et al. 1988). At low N concentrations when P_s tends to dominate, the average food-chain length would be greater because more of the zooplankton food supply would flow through a 2-step food chain (P_s to D to Z) because of the relatively low Z preference for P_s. At high N concentrations on the other hand, most of the food supply for Z would come directly from P_l, a 1-step food chain.

For both P_l and P_s, we defined N uptake and cell growth (or net photosynthesis, μ) to be dependent on the product of a maximum growth (or uptake) rate (μ_{max}) and hyperbolic functions of both light and N concentration. In this case, nutrient uptake is de-scribed with standard Michaelis-Menten kinetics and the light response uses an exponential saturation:

$$\mu = \mu_{max}[N/(N + K_N)][1 - \exp(-I/I_k)]P \qquad (2)$$

where K_N is the half-saturation coefficient for N uptake, I_k is the light saturation level, and I is the mean irradiance. Values for I were approximated as the vertical integration of an exponential light attenuation function over the mixed layer depth (z), divided by that depth (Stickney et al. 2000).

Losses from phytoplankton state variables included a first-order term for sinking and a quadratic term for algal senescence, whereby the latter provides a generic representation of density-dependent self-limitation. We set the sinking rates (e.g. Scavia et al. 1988, Moloney & Field 1991) and the zooplankton food-preference coefficients (e.g. Scavia et al. 1988, Andersen & Nival 1989) substantially higher for the large than the small phytoplankton (Table 1). We further distinguished between the physiology of P_l and P_s in this model by using distinctly different coefficients for key processes (Table 1). We set maximum growth rates at 3.05 d^{-1} for P_l and 0.80 d^{-1} for P_s, while half-saturation constants for the DIN uptake were 1.0 and 0.6 μM for P_l and P_s, respectively (e.g. Scavia et al. 1988, Andersen & Nival 1989). We assumed similar algal senescence rates of 0.12 d^{-1} for P_l and 0.10 d^{-1} for P_s (e.g. Moloney & Field 1991).

We also used the 2-compartment (P-Z) model to test the generality of our formulation for P self-limitation by replacing the quadratic algal senescence term with a self-shading expression in the algal growth term. Here, growth (μ) is described as follows:

$$\mu = \mu_{max}[N/(K_n + N)][I/z]P \qquad (3)$$

and

$$I/z = [I_o/kz](1 - e^{-kz}) \qquad (4)$$

where μ_{max}, and K_n are defined in Table 2 and Eq. (2), respectively, I_o is light at the water surface and k is the diffuse downwelling light attenuation coefficient. This light attenuation coefficient is further defined as $k = k_1 + k_2P$, implying that light absorption by phytoplankton cells (P) contributes substantially to total attenuation. This is a simple and traditional formulation that assumes that light is a limiting factor for algal

Table 2. Definition of terms and values used in base run for 5-compartment plankton model

Parameter	Symbol	Value	Units
Assimilation efficiency for Z on D	ξ_{a_D}	0.375	Dimensionless
Assimilation efficiency for Z on P_l	ξ_{a_l}	0.75	Dimensionless
Assimilation efficiency for Z on P_s	ξ_{a_s}	0.75	Dimensionless
Zooplankton preference for D	β_D	0.49	Dimensionless
Zooplankton preference for P_l	β_l	0.49	Dimensionless
Zooplankton preference for P_s	β_s	0.02	Dimensionless
Growth efficiency for Z on D	ξ_{g_D}	0.15	Dimensionless
Growth efficiency for Z on P_l	ξ_{g_l}	0.30	Dimensionless
Growth efficiency for Z on P_s	ξ_{g_s}	0.30	Dimensionless
Total irradiance	I	90.0	$W\,m^{-2}$
Light saturation parameter	I_k	75.0	$W\,m^{-2}$
Saturation constant for grazing by Z	K_z	1.10	μM
Saturation constant for N uptake by P_l	K_{n_l}	1.00	μM
Saturation constant for N uptake by P_s	K_{n_s}	0.60	μM
Predation on zooplankton	p_z	0.12	d^{-1}
Senescence rate for P_l	l_l	0.10	$(\mu M\,d)^{-1}$
Senescence rate for P_s	l_s	0.12	$(\mu M\,d)^{-1}$
Zooplankton maximum grazing rate	G_{max}	3.20	d^{-1}
Maximum growth rate for P_l	μ_{max_l}	3.05	d^{-1}
Maximum growth rate for P_s	μ_{max_s}	0.80	d^{-1}
Detritus recycling rate	r	0.30	d^{-1}
Partitioning of phytoplankton senescence	b	0.50	d^{-1}
Sinking rate for P_l	v_l	0.18	d^{-1}
Sinking rate for P_s	v_s	0.001	d^{-1}
Sinking rate for D	v_d	0.01	d^{-1}
Refuge from predation for P_l	α	0.01	μM
Inflows of P_l, P_s and Z	Q_{I_l}	0.001	$\mu M\,d^{-1}$
Inflow of N	Q_{I_N}	0.3	$\mu M\,d^{-1}$
Outflow of N, D, P_l, P_s and Z	Q_{O_N} (for N)	0.1 · N (for N)	$\mu M\,d^{-1}$
Initial value for N	–	0.01	μM
Initial values for D, P_l, P_s and Z	–	3	μM

photosynthesis (e.g. Riley 1946). Values for k_1 and k_2 were taken as 0.12 m^{-1} and 0.02 m^2 (mmol N)$^{-1}$, respectively (e.g. Parsons et al. 1979), and z was arbitrarily set at 30 m.

Zooplankton. Previous modeling studies have suggested that zooplankton mortality is a key process regulating ecosystem dynamics (Steele & Henderson 1992, Edwards & Brindley 1999), and we therefore focused considerable attention on this function in the present study. One zooplankton mortality function that we used was of the form Z^b. In the initial version of our model we employed this zooplankton 'closure' term with $b = 2$ to represent mortality resulting from cannibalism, from predators which are also dependent on Z, or from disease infection spread by inter-individual interactions (e.g. Steele & Henderson 1992). For other simulation experiments we also utilized lower powers for this mortality function ($b = 1.0, 1.25, 1.5$), and a hyperbolic mortality which saturates at high values of Z (e.g. Scheffer 1991).

We allowed zooplankton to consume 3 different foods (P_l, P_s, and D) according to a simple preference function (Table 1) that accounts for both relative availability and the percent of each food item in their diet (Scavia 1979, Stickney et al. 2000). We selected preference coefficients to reflect the well-established fact that zooplankton tend to select food based on particle size, so that large phytoplankton and detrital particles were consumed with equal preference, which was far greater than that for small algal cells (e.g. Scavia et al. 1988). In this function, the sum of the preference values for zooplankton feeding equals 1. We accounted for the nutritional value of the different algal cells versus detritus by using different growth (ξ_g) and assimilation (ξ_a) efficiencies, with the values for D being half those used for both P_l and P_s (e.g. Scavia et al. 1988, Andersen & Nival 1989). We set values for (ξ_g) and (ξ_a) at 0.30 and 0.75, respectively, for zooplankton consuming both groups of phytoplankton (Heinbokel 1978, Verity 1985). Zooplankton grazing on P_l ceases at densities below a threshold (α), indicating a low-density refuge from predation loss (e.g. Scavia 1979). Finally, we used a maximum zooplankton grazing rate of 3.20 d^{-1} (Stickney et al. 2000) and a predation rate on zooplankton of 0.12 d^{-1} (Fasham et al. 1990). Thus, although our model was structured so that mean food-chain length would be shorter under high nutrients, overall TTE would depend also on relative abundance of D because of differences in zooplankton feeding preference and assimilation efficiency values.

Detritus and nutrients. This model included organic nitrogen losses associated with phytoplankton senescence and zooplankton egestion and mortality in the detritus (D) compartment, which is meant to encompass both dissolved and particulate non-living organic matter. In addition, we also considered D to represent the bacteria associated with non-living organic matter, and therefore flows to and from D constitute a simplified 'microbial loop' (e.g. Steele 1998). We included bacterial metabolism as a first-order respiratory loss term from D; this loss also recycles nutrients back to N. Recycling of inorganic N also occurred via all respiratory pathways. The model partitions nitrogen losses from phytoplankton senescence into inorganic and organic fractions that are transferred to N and D compartments, respectively. Detritus is also lost from the model via sinking as a first-order loss term (e.g. Fasham et al. 1990). Inputs to organic (D) and inorganic (N) nitrogen from the zooplankton compartment are calculated using ξ_a and ξ_g for each potential food item. In this case, zooplankton egestion is computed as the amount of food not assimilated $(1 - \xi_a)$. The model considers zooplankton respiration and associated N recycling by the zooplankton as the amount of assimilated material which is not used for growth ($\xi_a - \xi_g$).

RESULTS AND DISCUSSION

Ecosystem responses to increasing nutrients

Temporal response

The 5-compartment model (N-P_l-P_s-Z-D) was run for a 300 d simulation at various mean N concentrations. Example time-courses are provided for relatively low (~2 µM), intermediate (~7 µM) and high (~12 µM) ambient N concentrations, which were regulated by adjusting concentrations of external N sources (Fig. 2). After initial transient behavior, biomass values achieved steady-state levels within 30 d at low and high nutrients; however, an oscillating pattern at intermediate concentrations continued beyond 100 d until it was internally damped. These cycling patterns indicate an underdamped system at intermediate nutrient conditions. At low N concentrations, total algal biomass was dominated by small phytoplankton; at intermediate nutrient levels, all model compartments increased, but P_s still dominated the phytoplankton biomass. At high N concentrations, large phytoplankton dominated, and there was a substantial increase in the amount of detritus in the system. The instability evident at the intermediate N concentrations occurred as the model approached a transition from a low N state dominated by P_s to a high N state dominated by P_l and D. This response to increasing N was completely consistent with expected competitive shifts between the 2 algal groups (e.g. Hecky & Kilham 1988) reflected in the model coefficients.
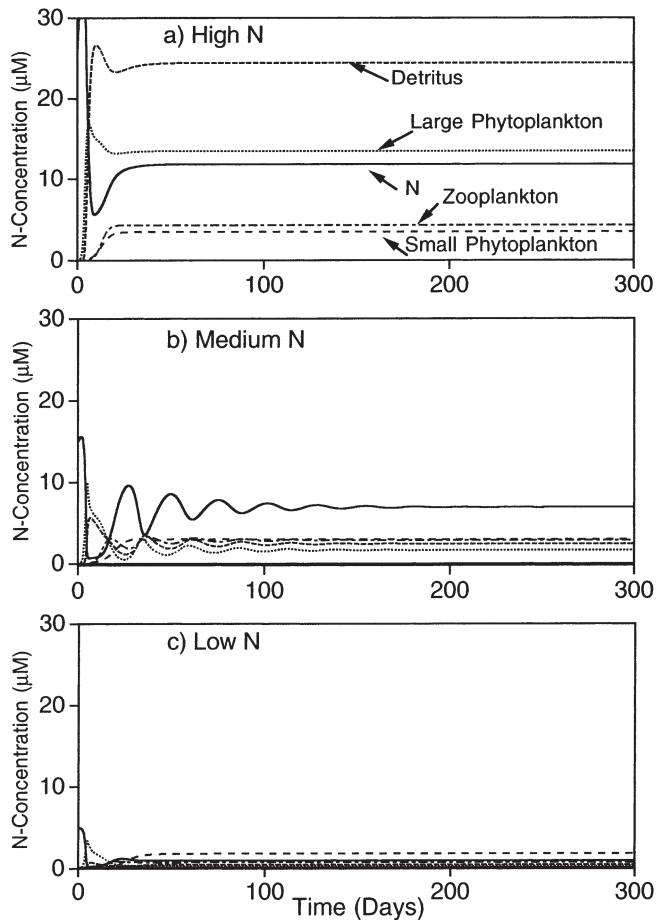
Fig. 2. Time-course simulation of 5-compartment pelagic eco-system model (Fig. 1d) under conditions of high, intermediate, and low nutrient input

Phase-shift responses and trophic efficiency

We explored this apparent shift in system state by running the model over a wide range of steady-state N concentrations from 1 to 15 µM (Fig. 3). With model parameter settings unchanged from calibration, we observed a dramatic shift in biomass and production levels and partitioning at N ≈ 7 µM (Fig. 3). It is clear from Fig. 3 that the steep shift was characterized by a transition from P_s dominance at low N to P_l and D dominance at higher N. Although D biomass exceeded that of P_l at high nutrient levels, growth of large algal cells was substantially greater than the rate of D production from mortality and excretion of P and Z. The relative significance of zooplankton also declined abruptly at the N transition, with the ratios $Z/(P_l + P_s)$ and Z/D both exhibiting dramatic decreases at the transition, although the former also showed a slight increase with increasing N before the transition point (Fig. 4a). The ratio of phytoplankton to detritus $[(P_l + P_s)/D]$ biomass declined more continuously over the entire N range,

with only a small drop at the transition point (Fig. 4b). The ratio of phytoplankton to detritus production, how-ever, declined up to the transition, at which point it jumped higher and continued to increase slightly with increasing N.

We were initially surprised to discover that the rela-tive importance of N recycling (as indicated by the ratio of exogenous inputs to recycling plus inputs) increased sharply with increasing N inputs from about 45 % at low N to 60 % at the state transition point. After this transition, the importance of recycling remained constant at about 70 % of total inputs to the N pool (Fig. 5). This contrasts with the concept that pelagic ecosystems tend to experience a steady decrease in the relative importance of nutrient recycling (to support primary production) along a gradient of increasing inputs of new nutrients (e.g. Nixon 1988, Eppley 1989). This apparent increase in relative recycling even as external inputs increase can be explained by the rela-tively closed nature of the model system compared to natural pelagic habitats. In the model, the increase in relative recycling with higher nutrient inputs resulted from accumulation rather than export of increasing detrital production (Fig. 4).

TTE of the model ecosystem responded strongly to changes in nutrient level, increasing from about 10 % at
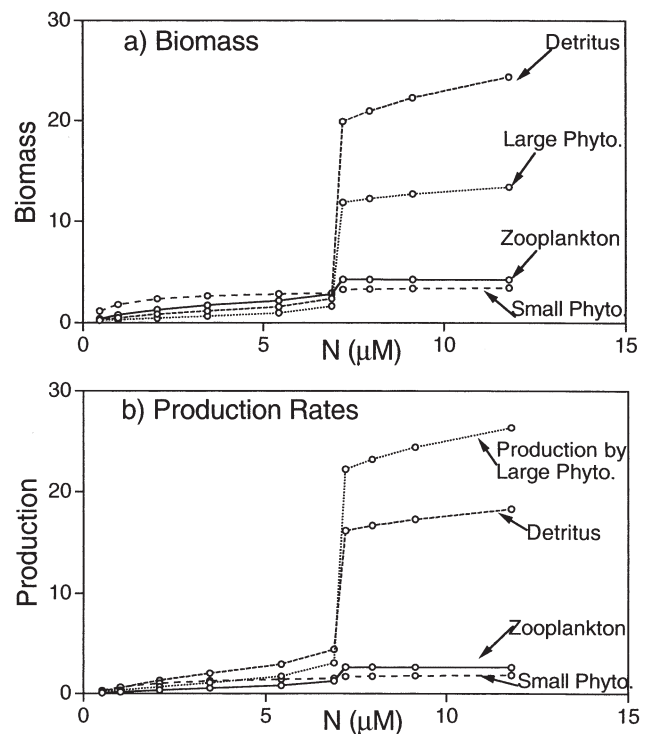

Fig. 3. Variations in biomass (µM) and production (µM d^{-1}) of phytoplankton, zooplankton and detritus as a function of changes in nutrient loading for 5-compartment pelagic ecosystem model (Fig. 1d). Note phase shift at N ≈ 7 µM
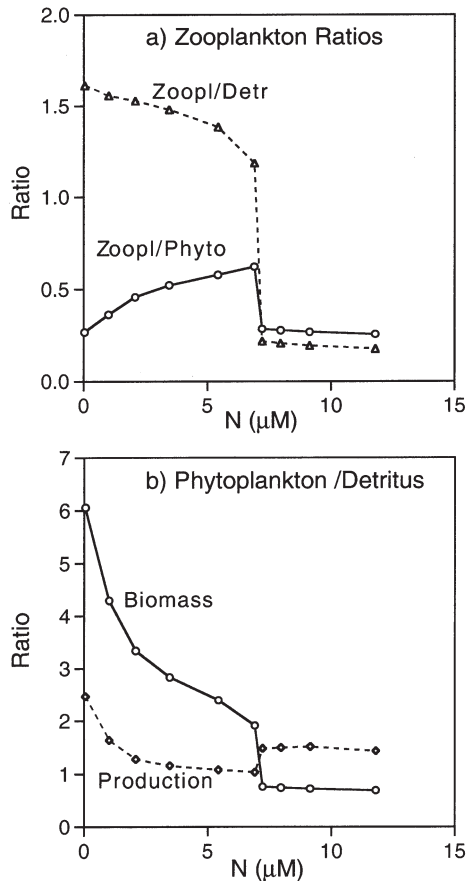
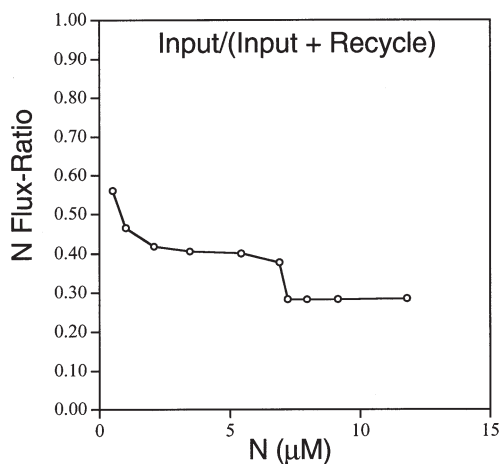Fig. 4. Variations in biomass ratios of zooplankton/phytoplankton and zooplankton/detritus and of phytoplankton/detritus biomass and production, as a function of changes in nutrient-loading for 5-compartment pelagic ecosystem model (Fig. 1d). Note phase shift at N ≈ 7 μM

low N to almost 30% at the transition point, at which TTE declined back to ~10% and remained relatively unchanged with increasing N (Fig. 6). Our initial interpretation was that the increasing TTE with N to the left of the transition point was attributable to the increased consumption of P_1 by Z, and the associated shortening of the average length of the food chain (e.g. Ryther 1969, Landry 1977). However, as we shall demonstrate below, the actual explanation lies in the effects of saturating resource utilization. In this case, the initial increase in TTE with increasing N resulted from saturation of nutrient uptake, while the abrupt decline in TTE at the transition point and the subsequent gradual decrease thereafter were related to saturation of zooplankton grazing control over algal biomass. The model experiences a steep transition to a new stable equilibrium state, as the grazing control on algae saturates and no longer controls P biomass. This phenomenon of phase shifts in phytoplankton-zooplankton interactions, which has been reported previously using simple 2-compartment (P-Z) and 3-compartment models (P-Z-fish), has been attributed to inherent instabilities or chaotic behavior of these systems (e.g. Rosenzweig 1971, Hastings & Powell 1991, Scheffer 1991). Some evidence from field experiments appears to support this general phase-shift pattern with nutrient enrichment (Scheffer 1991).

System complexity and TTE versus N

We investigated the generality of this modeled relationship between TTE and nutrient enrichment through

Fig. 5. Variations in ratio of external N-input to total flux of nitrogen input (external N input + N recycling) as a function of changes in nutrient concentration for 5-compartment pelagic ecosystem model (Fig. 1d). Note phase shift at N ≈ 7 μM
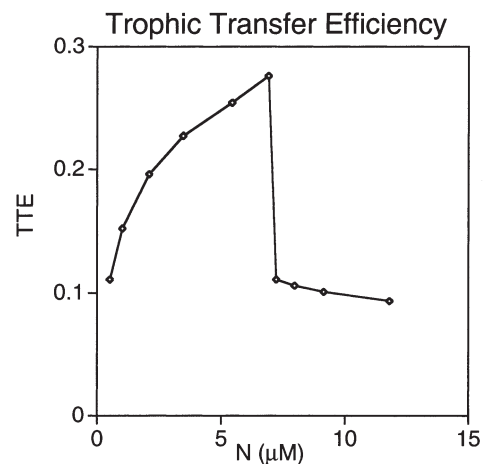

Fig. 6. Variations in trophic transfer efficiency (TTE, zooplankton growth per phytoplankton production) as a function of changes in nutrient concentration for 5-compartment pelagic ecosystem model (Fig. 1d). Note phase shift at N ≈ 7 μM

a series of numerical experiments and analyses. First, we conducted the same simulation series, recording variations in steady-state computations of TTE with increases in N for 4 different versions of this plankton ecosystem model, ranging from 2 to 5 compartments (Fig. 1). Clearly, all 4 models exhibited similar patterns, with the transitions becoming more abrupt and the phase-shift point moving toward higher values of N with increased model complexity (Fig. 7a). The relationships between TTE and N are scaled to maximum observed TTE to make results comparable. We surmise that the general shape of this relationship between TTE and N concentration may be robust, that it occurs in more complex ecosystem models and, as argued by previous investigators, that it may exist in nature (e.g. Scheffer 1991, Carpenter et al. 1995).

We further investigated the generality of the relationship between TTE and N by modifying the structure of the loss terms in the dP/dt equations. We had intended the quadratic loss term in the phytoplankton equations to serve as a generic representation of density-dependent self-limitation. This is consistent with the conventional interpretation of the quadratic loss term in the familiar 'logistic growth' equation commonly applied in describing population dynamics (e.g. Odum 1971). Here, growth is proportional to the population size and death is proportional to population squared (e.g. Haefner 1996). There are numerous self-limiting processes in natural populations, such as competition for space, disease transmission, and self-shading in plants, that arise when organism abundance is very high (e.g. Odum 1971). To test the generality of representing self-limitation with a quadratic loss for phytoplankton, we removed it and added instead an explicit representation of self-shading in the P growth term for the 2-compartment (P-Z) version of the model. Results of numerical experiments (Fig. 7b) reveal that, compared to the pattern with the quadratic loss term, TTE with self-shading exhibits a similar but less drastic decline at higher N loading.

The difference in steepness of the decline in TTE at higher N (Fig. 7) is related to the differences in the 2 ways that self-limitation was represented in the phytoplankton equation. In either case, the primary balance in the dP/dt equation is between phytoplankton growth and zooplankton grazing at low nutrient levels. As zooplankton grazing becomes satiated with increasing food levels, further increases in N loading drive the system toward a point where Z grazing can no longer control P. At this point the system moves, either gradually or sharply, toward a new equilibrium wherein phytoplankton growth is balanced by its own self-limitation rather than by Z grazing. In this case, the increased P production at higher N is shunted to detrital rather than grazing pathways, and TTE declines. The transi-
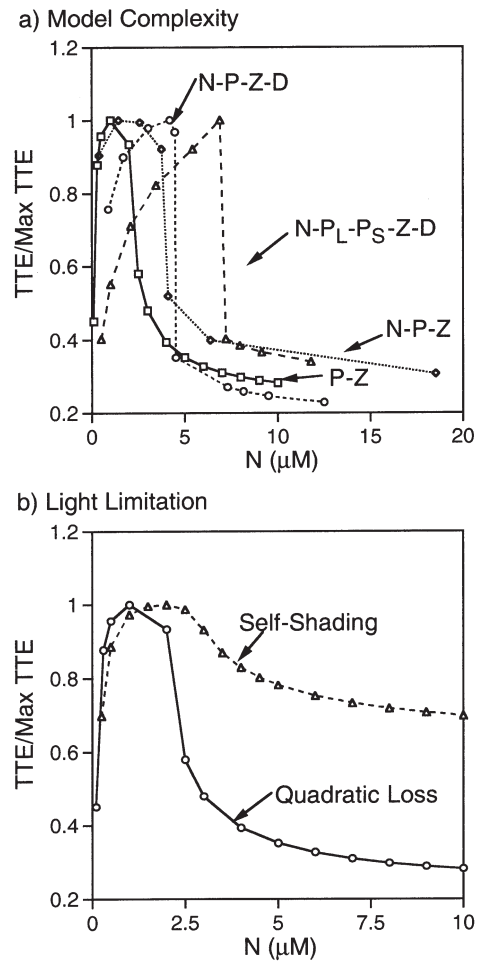

Fig. 7. Effects of model complexity and phytoplankton self-shading (light limitation) on the relationship between TTE and N concentration. In (a), each curve represents 1 of the 4 model configurations in Fig. 1; for comparison, relationships are scaled to respective maximum TTE in each case. Note that the phase-shift point changes with model complexity. In (b), the 2-compartment (P-Z) model illustrates contrasting effects of representing P self-regulation as a quadratic loss term (P^2) or by self-shading (see Eqs 3 & 4). Note scale differences on N axes

tion to lower TTE is more abrupt with the quadratic loss, because a large increase in P after release of grazing control is required before the quadratic mortality can balance increasing algal growth. In contrast, self-shading regulates P growth rather than mortality, and thus produces a more gradual shift and associated decline in TTE with increased N.

Grazing, mortality and kinetic controls on TTE versus N

To test the mechanisms behind the observed relationships between TTE and N, we conducted numerical experiments using the simplest 2-compartment version

of the model (Fig. 1a). Our first test involved changing the zooplankton feeding function from a saturating hyperbolic equation to a linear, first-order equation. The result was to retain the increases in TTE with N at low nutrients but to remove completely the phase shift (Fig. 8a), thereby producing a relationship similar to that derived from analysis of data on marine phytoplankton production and fisheries harvests (Iverson 1990). This numerical experiment, however, corroborates our interpretation that the sharp decline in the relationship between TTE and N is attributable to the saturation of zooplankton control on phytoplankton.

We also tested the response to variations in the structure of the closure or mortality term for zooplankton using 4 different formulations (Fig. 8b). For all closure formulations, we adjusted coefficients such that total mortality rates were similar over the experimental range (e.g. Caswell & Neubert 1998). Two of the closure terms presented are power functions of the form $m_z Z^b$, where m_z is a mortality rate coefficient and b is equal to 1.5 and 2.0. These power functions tend to exert relatively strong top-down control because the predators never saturate, and they respond instantly to increases in the Z population. With $b > 1.0$, biomass-specific mortality rate increases with biomass. With $b = 2.0$, this closure can be interpreted as cannibalism, disease or mortality resulting from predators which are also dependent on Z (Steele & Henderson 1992). The quadratic closure leads to abrupt catastrophic decline in TTE at a phase-shift point. The 1.5 power function, however, produced a relatively smooth (non-bifurcating) transition from lower to higher to lower values of TTE as N increases (Fig. 8b), and an even more gradual decline in TTE at higher N was evident with $b = 1.25$ (not shown). Hence, it appears that, contrary to previous discussions (e.g. Rozensweig 1971, Scheffer 1991), this general pattern is not exclusive to models with inherently unstable or chaotic equation structures. With simple first-order closure, this model exhibited a highly unstable behavior (not shown) similar to previous reports (e.g. Steele & Henderson 1992). We acknowledge that such instabilities may occur regardless of the closure formulation (Caswell & Neubert 1998).

We also used hyperbolic saturation functions of the form $Z^c(K_Z + Z^c)^{-1}$ to describe zooplankton mortality, where K_Z is a grazing half-saturation coefficient and the exponent c was equal to 1 and 2 (Fasham et al. 1990, Scheffer 1991). These equations describe a saturating mortality rate resulting from a satiable predator, and the sigmoidal function ($c = 2$) simulates a refuge from predation at low Z (e.g. Holling 1959). With both forms of saturating closure, top-down control is exerted only when Z is low relative to K_Z. With hyperbolic closure ($c = 1$), there was no decline in TTE at higher nutrient levels, while with the sigmoidal closure ($c = 2$),
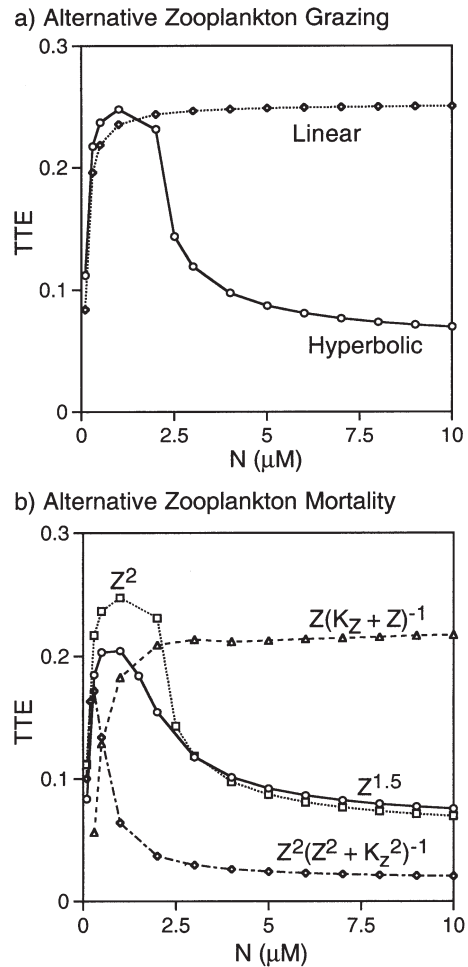

Fig. 8. Effects of alternative zooplankton grazing equations and alternative zooplankton mortality functions on the relationship between TTE and N in the 2-compartment pelagic ecosystem model (Fig. 1a). Note that the phase shift disappears with linear grazing and hyperbolic mortality

the shift was dramatic, but occurred at very low values of N and Z (Figs 3 & 8b). These experiments demonstrate that, while model formulations representing more intense predation mortality for zooplankton produced declining trophic efficiency at high N, TTE saturated at high N for equations representing less intense (zero to first-order) top-down control.

It can be shown numerically and analytically that the initial increase in TTE at low N is the result of an increase in P growth rate relative to the advection/sinking loss rate, and that the N concentration where maximum TTE and subsequent decline occurs is inversely related to the half-saturation constant for N uptake, K_N (Figs 6 to 8). For simplicity, we illustrate these points using the 2-compartment (P-Z) model, in which N is described as a forcing function. Furthermore, for this analysis we assume that, at low concentrations of N,

the quadratic loss term for P is negligible and zoo-plankton grazing is a first-order function of P. Thus, the equations describing this P-Z model are as follows:

$$dP/dt = \mu_{max} P[N/(N + K_n)] - G_{max} Z P - v P \quad (5)$$

$$dZ/dt = \xi_g G_{max} Z P - v Z - p_Z Z^b \quad (6)$$

where μ_{max} and G_{max} are maximum growth rates for phytoplankton (P) and grazing rates for zooplankton (Z), respectively, ξ_g is the growth efficiency for Z, K_N is the half-saturation coefficient for N uptake by P, v is the sinking/advection rate for P and Z, and p_z is the rate coefficient for predation on Z. As before (Eq. 1), we define the TTE as the ratio of the first terms on the respective right-hand sides of Eqs (5) and (6):

$$TTE = [\xi_g G_{max} Z]\{\mu_{max}[N/(N + K_N)]\}^{-1} \quad (7)$$

Next, we compute the steady-state solution to Eq. (6) for Z and substitute it back into Eq. (7) to obtain the following expression for TTE at low N (TTE_i):

$$TTE_i = \xi_g\{1 - v/\mu_{max}[N/(N + K_P)]\} \quad (8)$$

With the parameters in Eq. (8) (ξ_g, v, μ_{max}, K_P) held constant, the expression describes TTE_i as a hyperbolic function of N. This analytical solution illustrates that the trophic efficiency at low N directly depends both on the zooplankton growth efficiency and on 1 minus the ratio of sinking/advection to phytoplankton growth rate. Thus, increases in algal sinking or flushing rates will also tend to decrease trophic efficiency by reducing the access of secondary consumers to primary production.

We used numerical sensitivity experiments on this 2-compartment (P-Z) model to investigate how kinetic parameters for nutrient uptake and zooplankton grazing influence the shape of the relationship between TTE and N. In general, we found that changes in the half-saturation coefficients both for P uptake of N (K_N) and for Z grazing on P (K_Z) resulted in substantial shifts in the point along the N gradient where TTE began to decline (Fig. 9). In contrast, changes in the initial slope of this TTE-N relationship were negligible. Increases in K_N tended to move the point of TTE decline to higher N concentrations without changing the shape of the relationship (Fig. 9a). Increases in K_Z, however, resulted in complex, non-linear changes in the shape and position of this TTE-N relationship (Fig. 9b).

Trophic responses to resource variability

We also considered the effect of introducing variability in resource availability into this aquatic ecosystem model. We examined this question first at the level of the whole ecosystem, and then looked more closely at

the level of the grazer population. To simulate resource variability, we added a fluctuating component to the model's N supply, while maintaining the same mean concentrations. The time-course model solutions did not change dramatically with variable (Fig. 10) versus constant (Fig. 2) N input. At low concentrations of N, phytoplankton were dominated by P_s and the biomasses were generally low, while at high N concentrations the system biomass becomes dominated by P_l and D. At intermediate N concentrations, we saw evidence of instabilities contributing to relatively greater oscillations in model components. There were other interesting patterns in the time-course simulation (Fig. 10), where the dominant period of variation in the N pool appears to have increased with mean N (Fig. 10: left-hand graphs). The relative variability in P_l, P_s, and Z appears to have been damped with increasing mean N
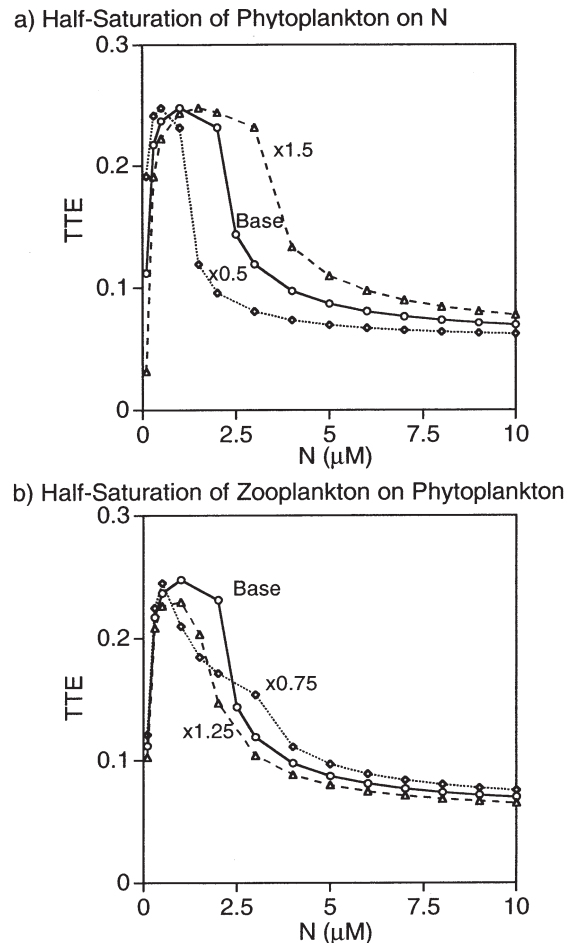

Fig. 9. Effects of changing half-saturation coefficients for phytoplankton uptake of N (a) and zooplankton grazing on phytoplankton (b) on the relationship between TTE and N in the 2-compartment pelagic ecosystem model (Fig. 1a). Note that the phase-shift point changes with variations in half-saturation coefficients
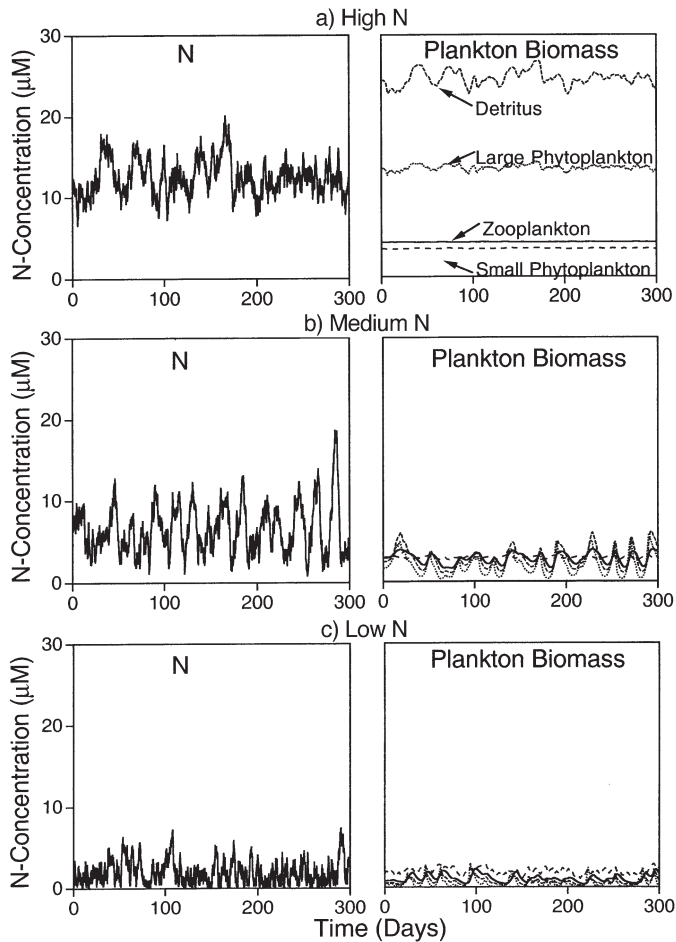
Fig. 10. Time-course simulation of 5-compartment pelagic ecosystem model (Fig. 1d) under conditions of variable N-input at high, medium and low nutrient-loading rates

(results not shown). A number of previous modeling studies have demonstrated that frequency of variation in resource availability can influence plankton responses (e.g. Powell & Richerson 1985, Davis et al. 1991). In general, it appears that plankton assemblages are most responsive to variabilities in resource availability when the ratio of biological time-scale (e.g. biomass turnover time) to physical time-scale (i.e. dominant frequency of resource variation) approaches unity (e.g. Kemp & Mitsch 1979, Anderies & Beisner 2000). In this analysis, however, we did not investigate how different frequencies of variation might affect trophic efficiencies in the model plankton communities. Here, variations were all done at the frequency of the numerical time-step (0.1 d).

We also focused this analysis below the level of the integrated pelagic ecosystem to that of an isolated consumer population (Z), where changes in mean and variance of nutrient resources were assumed to be reflected as variations in algal biomass. In this case, we defined the ratio of zooplankton consumption to phytoplankton input (TTE_Z) as a proxy for TTE, assuming constant values for phytoplankton growth rate and zooplankton growth efficiency ($\xi_g = 1$). Although TTE_Z is determined both by the herbivore growth efficiency and by the functional response of the herbivore to its prey, we focus here on the functional response relationship. For generality, we used a Holling Type III function of the form $G = G_{max}[P^2/(P^2 + K_Z^2)]$ to describe zooplankton grazing (Holling 1959). We consider this sigmoidal function to be more general than a hyperbolic function (e.g. Scheffer 1991), because it contains refuge from grazing at low P concentrations where consumption approaches zero (Holling 1959).

level; however, D seems to have retained its variance despite the nutrient conditions (Fig. 10: right-hand graphs). Although the introduction of variability did not fundamentally change the relationship between N concentration and TTE described above (Fig. 6), it tended to enhance TTE at low nutrient concentrations (Fig. 11). Variability in N also appears to have moved the transition point to the right and decreased TTE at intermediate concentrations (Fig. 11). This relatively complex mixture of trophic responses to variable resource levels is similar to previous reports from theoretical and empirical studies (e.g. Davis et al. 1991).

This modest enhancement of TTE with variable nutrient resources at low N is attributable to the ability of large phytoplankton to exploit pulsed increases in N because of their higher growth rates and kinetic saturation values (Table 2). Under these conditions, increases in the ratio of P_l to P_s result in shorter average food chains, and hence higher values for TTE. In fact, we saw negligible effects of variance on TTE using the 4-compartment model with only 1 phytoplankton group
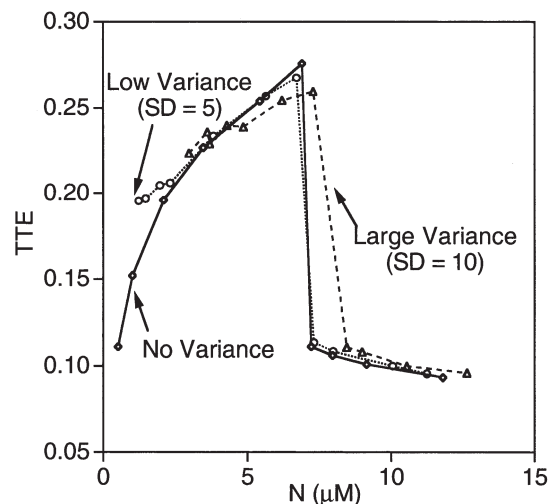

Fig. 11. Variations in relationship between TTE and N concentration in 5-compartment pelagic ecosystem model (Fig. 1d) for conditions of no variance in N and low (SD = 5) and high (SD = 10) variance

We generated a series of normal phytoplankton biomass distributions with different means and variances and then 'transformed' them using the feeding function with K_Z set at 1 and G_{max} at 3 d^{-1}. This procedure is analogous to non-linear, statistical transformations, such as the log transformation, which are commonly employed to change the shape of a distribution to make it more normal. In this case we are applying the feeding function as a transformation to a series of normally distributed phytoplankton inputs. These inputs are 'transformed' using the Type III grazing function to generate zooplankton growth rate distributions, which tend to diverge from normality because the transformation is non-linear.

We ran 42 different combinations of mean and standard deviation of phytoplankton availability (7 means, each with 6 different SD values). Frequency distributions of zooplankton growth rates (equivalent to grazing rates G when $\xi_g = 1$) were computed with the grazing function based on this phytoplankton input series (Fig. 12). It is evident that the frequency distributions tend to flatten and move to the right of the origin with increasing variance at relatively low values of P (Fig. 12: upper 3 graphs). At intermediate values of phytoplankton biomass (P = K_Z = 1), increased variance flattened the distributions but had little effect on the mean value (Fig. 12: middle 3 graphs). At relatively high values of P, increased variance resulted in pronounced flattening of distributions and skewing left toward the origin (Fig. 12: bottom 3 graphs).

The ratio of zooplankton growth to phytoplankton input (TTE$_Z$) exhibited a clear pattern (Fig. 13), with TTE$_Z$ increasing as mean values of P declined down to P = $0.5K_Z$, where variations were more complex. At higher values of P, increasing variance tended to cause a decrease in TTE$_Z$; however, at low values of P (oligotrophic conditions), increased variance caused substantial increases in TTE$_Z$ until the SD approached 1.0 (Fig. 13). At relatively low variance (SD < 0.5: Fig. 13), results were similar to those observed with resource inputs held constant (Fig. 6), where increasing resources resulted in an initial elevation of trophic efficiency followed by a decline in efficiency under mesotrophic to eutrophic conditions. This decline was, however, more gradual than that observed at the ecosystem level because P levels were prescribed in this analysis and therefore could not increase as saturating consumption released them from grazing pressure. We conducted a similar set of numerical experiments using a simple hyperbolic feeding function of the form $G = G_{max}[P/(P + K_Z)]$. In this case, the pattern was more consistent, with trophic efficiency declining with increased variance regardless of the level of P (results not shown).

These model results suggest that, for aquatic systems dominated by herbivores that cease grazing at low food concentrations, the effect of resource variability on trophic efficiency depends upon the nutrient conditions of the ecosystem. Variability in food supplies associated with, for example, nutrient pulses or physical discontinuities (e.g. Legendre & Demers 1984) can substantially enhance TTE (i.e. by 25 to 100%), but only at very low resource concentrations (Figs 11 & 13). As mean food concentrations increase, the benefit imparted by variability rapidly diminishes and can actually reduce trophic efficiency at intermediate to high resource concentrations.

Under eutrophic conditions, model variance produced reductions in trophic efficiency at the organism level and had little effect at the ecosystem level (Figs 11 & 13). As was the case at the ecosystem level for simulated conditions of constant high nutrient inputs (Fig. 6), this decrease in trophic efficiency with abundant but variable resource levels (Fig. 13) arises from grazing saturation. In this case, zooplankton growth does not respond to spikes of high phytoplankton abundance, and thus efficiency does not increase. In fact, this decline in trophic efficiency resulting from
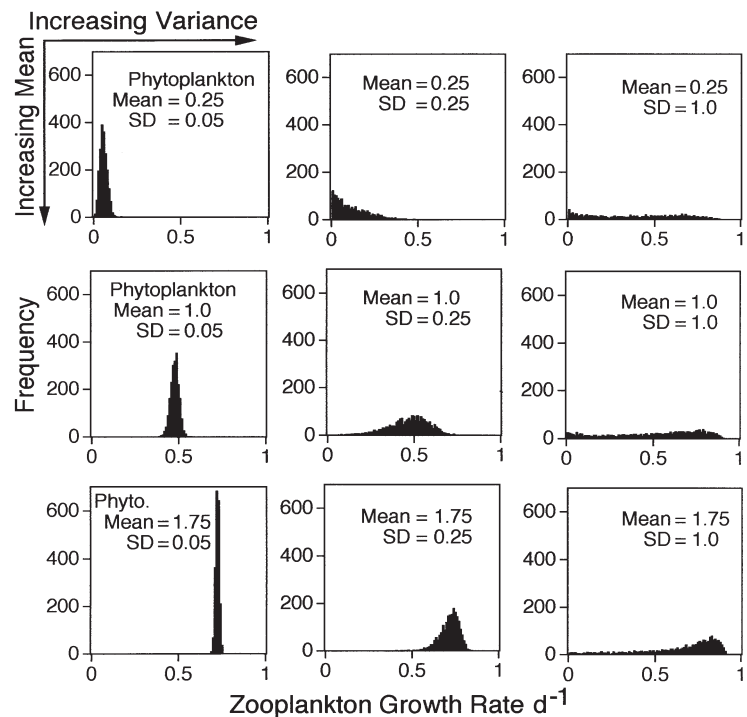

Fig. 12. Effects of changes in frequency distributions of variable phytoplankton (P) input (normal distributions, different mean and variance) on zooplankton growth using Type III feeding function; frequencies are number of values (bin size 0.01 d^{-1}) for 2000 random input values of P
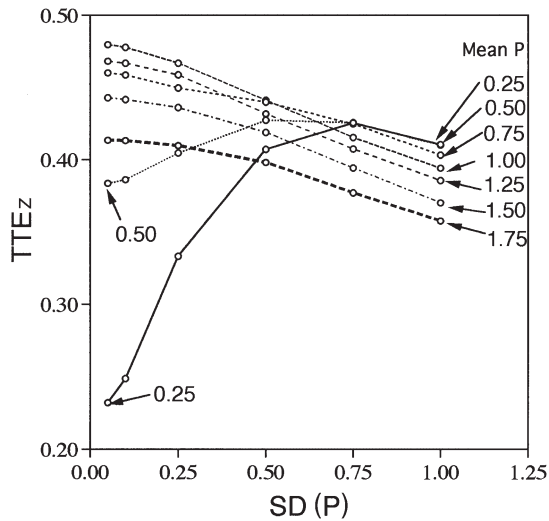
Fig. 13. Summary of effects of variance in phytoplankton availability on TTE_z (ratio of zooplankton grazing to phytoplankton input); here we consider interacting effects of changes in both mean (family of curves) and standard deviation (*x*-axis) of phytoplankton distributions

saturating consumption is the underlying mechanism that links our results observed at both ecosystem and organism levels and under conditions of both constant and variable resources.

Concluding comments

Our model analyses revealed that changes in nutrient concentrations tend to alter, in non-linear ways, the efficiency by which primary production is transferred to secondary consumers, as a result of fundamental relationships in pelagic ecosystems. Under oligotrophic conditions, small increases in nutrient levels lead to elevated trophic efficiency as algal biomass accumulates, herbivore access to primary production is improved, and physical losses become relatively less important. This observed pattern under low-to-moderate nutrient conditions is consistent with a recent report empirically relating the ratio of fisheries harvest to primary production versus 'nutrient level', as reflected in total phytoplankton production (Iverson 1990). However, the present modeling results also suggest that, under certain conditions, there is a critical point above which further increases in nutrient loading may lead to reductions in trophic efficiency. This pattern of declining transfer efficiency under eutrophic conditions appears to depend on the intensity of top-down control at the highest consumer trophic level. When grazer mortality functions reflect modest control (e.g. zero-order or first-order loss terms), trophic efficiency saturates at moderate nutrient levels. In contrast, when this closure

term in ecosystem models represents 'intense' predator control (i.e. prey-specific mortality increases with prey abundance), eutrophication leads to decreased trophic efficiency as grazing saturates and most of the production is shunted to detritus. In the latter case, the overall relationship between trophic efficiency and nutrient inputs exhibits 'diminishing returns' beyond moderate enrichment.

For certain fisheries, harvest pressure could be described as 'intense' in these mathematical terms because, for example, fishing fleets tend to aggregate on the richest fishing grounds (e.g. Royce 1972). Thus, we can speculate that for many highly managed coastal ecosystems and lakes simultaneous eutrophication and intense fishing pressure might lead to declining efficiency of transfer from primary production to fish harvest. Indeed, there are many anecdotal observations of decreasing herbivore abundance (e.g. Lehman 1988, Edmundson 1991) and fisheries production (e.g. Nelson 1958, Beeton 1969, Caddy 1993, Zaitsev 1993) associated with eutrophication of lakes and estuaries. The theory of 'trophic cascades' (e.g. Carpenter et al. 1985) suggests that intense predator control at an upper trophic level will result in relaxed top-down control at the next lower level which will, in turn, generate intense control at the trophic level below, and so on. In this case, trophic efficiencies at successive trophic levels may exhibit alternating responses to nutrient enrichment because of differences in the intensity of top-down control (e.g. Fig. 8b). The present results suggest that heavily exploited consumer organisms at any trophic level will, however, experience declining trophic efficiency, regardless of their position in a food-chain. Obviously, systematic empirical descriptions of relationships between TTE and nutrient enrichment would be useful to further our understanding of these fundamental relationships.

The scientific and management implications of the general relationships described here between trophic efficiency and nutrient input are obvious and profound. At low-to-moderate nutrient enrichment levels, pelagic ecosystems can efficiently support relatively high fish production. Considering only trophic dynamics (without regard for population dynamics), this lower-nutrient relationship would be unaffected by the nature of the fishing pressure. As nutrient enrichment progresses from mesotrophic to eutrophic conditions, however, the relative efficiency by which fish growth is supported by primary production may decline with further enrichment, if fishing pressure is intense. The widespread coincidence of eutrophication and highly exploited fisheries in coastal waters (e.g. Caddy 1993) suggests that this latter condition is commonplace. These modeling results are completely consistent with the marine ecosystem structures hypothesized to have

existed before the advent of intense human exploitation of fish populations (Steele & Schumacher 2000).

Previous studies have suggested that major changes in trophic efficiencies may arise with eutrophication via several mechanisms, including alterations in species composition (and attendant nutritional value) of phytoplankton and zooplankton (e.g. Landry 1977, Scavia et al. 1988). In addition, there are numerous reports of eutrophication-induced degradation of habitat conditions in lakes (e.g. Likens 1972) and estuaries (e.g. Nixon 1995). Changes in phytoplankton species from large nutritious cells to smaller unpalatable algae has been shown to often accompany increases in nutrients, particularly when nutrient increases are not stoichiometrically balanced among phosphorus, nitrogen and silica (e.g. Sanders et al. 1987, Hecky & Kilham 1988, Paerl 1988, Turner & Rabalais 1994). The large declines in plankton trophic efficiency at high nutrient levels in our model studies were, however, not associated with changes in species composition or habitat; rather, they resulted from grazing saturation. Furthermore, when increased primary production is not efficiently consumed by zooplankton, organic detritus tends to be shunted to decomposition processes, sometimes leading to depletion of dissolved oxygen (e.g. Officer et al. 1984). These hypoxic conditions tend to degrade animal habitats, thereby further reducing trophic efficiency. Because each of these complex ecological mechanisms associated with eutrophication tends to decrease trophic efficiency, their effects would simply add to the decline shown here to result from consumer saturation under nutrient-enriched conditions.

Our simulation experiments with pelagic ecosystem models incorporating intense top-down control exhibited dramatic declines in trophic efficiency with increasing nutrients at N concentrations between 2 and 7 μM, depending on model complexity (Figs 6 & 7). It remains an open question as to where such transition points might occur along a nutrient-enrichment scale in natural ecosystems. It is also unclear how one might recognize an approaching transition as an ecosystem undergoes progressive eutrophication. These are fundamental questions of aquatic science that have substantial implications for effective management of coastal ecosystems. In retrospect, many of the ideas generated in this study seem obvious, and we are surprised that there has been so little empirical and theoretical research focused on this basic topic. It seems to us that this is a subject that should be clearly understood and described in our scientific text books, as well as deeply ingrained into the way that human societies manage estuaries and other aquatic ecosystems.

LITERATURE CITED

Anderies JM, Beisner BF (2000) Fluctuating environments and phytoplankton community structure: a stochastic model. Am Nat 155:556–569

Andersen V, Nival P (1989) Modelling of phytoplankton population dynamics in an enclosed water column. J Mar Biol Assoc UK 69:625–646

Beeton AM (1969) Changes in the environment and biota of the Great Lakes. In: Rohlich GA (ed) Eutrophication: causes, consequences, correctives. National Academy of Science, Washington, DC, p 150–187

Caddy JF (1993) Towards a comparative evaluation of human impact on fishery ecosystems of enclosed and semi-enclosed seas. Rev Fish Sci 1:57–95

Carpenter SR, Kitchell JF (1984) Plankton community structure and limnetic primary production. Am Nat 124:159–172

Carpenter SR, Kitchell JF, Hodgson JR (1985) Cascading trophic interactions and lake productivity. BioScience 35: 634–639

Carpenter SR and 11 others (1995) Biological control of eutrophication in lakes. Environ Sci Technol 29:784–786

Caswell H, Neubert NG (1998) Chaos and closure terms in plankton food chain models. J Plankton Res 20:1837–1845

Dagg M (1977) Some effects of patchy food environments on copepods. Limnol Oceanogr 22:99–107

Davis CS, Flierl G, Wiebe P, Franks P (1991) Micropatchiness, turbulence and recruitment in plankton. J Mar Res 49: 109–151

Edmondson WT (1991) The uses of ecology. Lake Washington and beyond, University of Washington Press, Seattle, WA

Edwards AM, Brindley J (1999) Zooplankton mortality and the dynamical behaviour of plankton population models. Bull Math Biol 61:303–339

Eppley RW (1989) New production: history, methods, problems. In: Berger W, Smetacek V, Wefer G (eds) Productivity of the ocean: present and past. John Wiley, New York, p 85–97

Fasham MJR, Ducklow HW, McKelvie SM (1990) A nitrogen-based model of plankton dynamics in the oceanic mixed layer. J Mar Res 48:591–639

Haefner JW (1996) Modeling biological systems. Chapman & Hall, New York

Hastings A, Powell T (1991) Chaos in a three-species food chain. Ecology 72:896–903

Hecky RE, Kilham P (1988) Nutrient enrichment of phytoplankton in freshwater and marine environments: a review of recent evidence on effects of enrichment. Limnol Oceanogr 33(4, Part 2):796–822

Heinbokel JF (1978) Studies on the functional role of tintinnids in the Southern California Bight. I. Grazing and growth rates in laboratory cultures. Mar Biol 47:177–189

Holling CS (1959) Some characteristics of simple types of predation and parasitism. Can Entomol 91:385–398

Iverson RL (1990) Control of marine fish production. Limnol Oceanogr 35:1593–1604

Kemp WM, Mitsch WJ (1979) Turbulence and phytoplankton diversity: a general model of the paradox of plankton. Ecol Model 7:201–222

Landry MR (1977) A review of important concepts in the

trophic organization of pelagic ecosystems. Helgol Wiss Meeresunters 30:8–17

Legendre L, Demers S (1984) Towards dynamic biological oceanography and limnology. Can J Fish Aquat Sci 41: 2–19

Lehman JT (1988) Hypolimnetic metabolism in Lake Washington: relative effects of nutrient load and food web structure on lake productivity. Limnol Oceanogr 33(6, Part 1): 1334–1347

Likens GE (ed) (1972) Nutrients and eutrophication: the limiting nutrient controversy. Spec Symp Am Soc Limnol Oceanogr, Vol. 1, Allen Press, Lawrence, KA

Mackas DL, Denman KL, Abbott MR (1985) Plankton patchiness: biology in the physical vernacular. Bull Mar Sci 37: 652–664

Moloney C, Field J (1991) The size-based dynamics of plankton food webs. I. A simulation model of carbon and nitrogen flows. J Plankton Res 13:1003–1038

Nelson PR (1958) Relationship between rate of photosynthesis and growth of juvenile red salmon. Science 128:205–206

Nixon SW (1988) Physical energy inputs and the comparative ecology of lake and marine ecosystems. Limnol Oceanogr 33:1005–1025

Nixon SW (1995) Coastal marine eutrophication: a definition, social causes, and future concerns. Ophelia 41:199–219

Odum EP (1971) Fundamentals of ecology, 3rd edn. Saunders, Philadelphia, PA

Officer CB, Biggs RB, Taft JL, Cronin LE, Tyler MA, Boynton WR (1984) Chesapeake Bay anoxia: origin, development and significance. Science 23:22–27

Oglesby RT (1977) Relationships of fish yield to lake phytoplankton standing crop, production and morphoedaphic factors. J Fish Res Board Can 34:2271–2279

Pace ML, Glasser JE, Pomeroy LR (1984) A simulation model analysis of continental shelf food webs. Mar Biol 82: 47–63

Paerl HW (1988) Nuisance phytoplankton blooms in coastal, estuarine, and inland waters. Limnol Oceanogr 33(4, Part 2): 796–822

Parsons TR, Takahashi M, Hargrave B (1979) Biological - oceanographic processes, 2nd edn. Pergamon Press, Oxford

Pauly D, Christensen V (1995) Primary production required to sustain global fisheries. Nature (Lond) 374:255–257

Pauly D, Christensen V, Dalsgaard J, Froese R, Torres F (1998) Fishing down the food chain. Science 279:860–863

Powell T, Richerson PJ (1985) Temporal variations, spatial heterogeneity, and competition for resources in plankton systems: a theoretical model. Am Nat 125:431–464

Rosenzweig ML (1971) Paradox of enrichment: destabilization of exploitation ecosystems in ecological time. Science 171: 385–387

Ross AH, Gurney W, Heath M (1993a) Ecosystem models of Scottish sea lochs for assessing the impact of nutrient enrichment. ICES J Mar Sci 50:359–367

Ross AH, Gurney W, Heath M, Hay S, Henderson E (1993b) A strategic simulation model of a fjord ecosystem. Limnol Oceanogr 38:128–153

Royce WF (1972) Introduction to the fishery science. Academic Press, New York

Riley GA (1946) Factors controlling phytoplankton populations on Georges Bank. J Mar Res 6:54–73

Ryther JH (1969) Photosynthesis and fish production in the sea. Science 166:72–76

Saiz E, Tiselius P, Jonsson P, Verity P, Paffenhöfer G (1993) Experimental records of the effects of food patchiness and predation on egg production of *Acartia tonsa*. Limnol Oceanogr 38:280–289

Sanders J, Cibik S, D'Elia C, Boynton W (1987) Nutrient enrichment studies in a coastal plain estuary: changes in phytoplankton species composition. Can J Fish Aquat Sci 44:83–90

Scavia D (1979) The use of ecological models of lakes in synthesizing available information and identifying research needs. In: Scavia D, Robertson A (eds) Perspectives on lake ecosystem modeling. Ann Arbor Science, Publishers Inc, Ann Arbor, MI, p 109–168

Scavia D, Lang GA, Kitchell JF (1988) Dynamics of Lake Michigan plankton: a model evaluation of nutrient loading, competition and predation. Can J Fish Aquat Sci 45: 165–177

Scheffer M (1991) Fish and nutrients interplay determines algal biomass: a minimal model. Oikos 62:271–282

Steele JH (1998) Incorporating the microbial loop in a simple plankton model. Proc R Soc Lond Ser B Biol Sci 265: 1771–1777

Steele JH, Henderson EW (1992) The role of predation in plankton models. J Plankton Res 14:157–172

Steele JH, Schumacher M (2000) Ecosystem structure before fishing. Fish Res (Amst) 44:201–205

Stickney HL, Hood R, Stoecker D (2000) The impact of mixotrophy on planktonic marine ecosystems. Ecol Model 125:203–230

Tiselius P, Jonsson P, Verity P (1993) A model evaluation of the impact of food patchiness on foraging strategy and predation risk in zooplankton. Bull Mar Sci 53:247–264

Totterdell I (1993) An annotated bibliography of marine biological models. In: Evans G, Fasham M (eds) Towards a model of ocean biogeochemical processes. Springer-Verlag, Berlin, p 317–339

Turner RE, Rabalais N (1994) Coastal eutrophication near the Mississippi River delta. Nature (Lond) 368:619–621

Verity PG (1985) Grazing, respiration, excretion and growth rates of tintinnids. Limnol Oceanogr 30:1268–1282

Zaitsev Y (1993) Impacts of eutrophication on the Black Sea fauna. Stud Rev Gen Fish Counc Mediterr (FAO) 64:63–86